Dalton Transactions

Accepted Manuscript

This article can be cited before page numbers have been issued, to do this please use: B. Godde, A. Jouaiti, A. Fluck, N. Kyritsakas, M. Mauro and M. W. Hosseini, *Dalton Trans.*, 2017, DOI: 10.1039/C7DT02762A.

This is an Accepted Manuscript, which has been through the Royal Society of Chemistry peer review process and has been accepted for publication.

Accepted Manuscripts are published online shortly after acceptance, before technical editing, formatting and proof reading. Using this free service, authors can make their results available to the community, in citable form, before we publish the edited article. We will replace this Accepted Manuscript with the edited and formatted Advance Article as soon as it is available.

You can find more information about Accepted Manuscripts in the author guidelines.

Please note that technical editing may introduce minor changes to the text and/or graphics, which may alter content. The journal's standard Terms & Conditions and the ethical guidelines, outlined in our author and reviewer resource centre, still apply. In no event shall the Royal Society of Chemistry be held responsible for any errors or omissions in this Accepted Manuscript or any consequences arising from the use of any information it contains.

ROYAL SOCIETY OF CHEMISTRY

rsc.li/dalton

View Article Online
DOI: 10.1039/C7DT02762A

Journal Name

ARTICLE

Received 00th January 20xx,

Accepted 00th January 20xx

DOI: 10.1039/x0xx00000x

www.rsc.org/

Symmetrical or non-symmetrical luminescent turnstiles based on hydroquinone stators and rotors bearing pyridyl or *p*-dimethyaminopyridyl coordinating units

Bérangère Godde, Abdelaziz Jouaiti,* Audrey Fluck, Nathalie Kyritsakas, Matteo Mauro,* and Mir Wais Hosseini*

The design and synthesis of a novel family of molecular turnstiles T1-T5 were achieved. All five turnstiles are based on a stator and a rotor covalently interconnected. Whereas turnstiles T1-T2 are based on a symmetric stator equipped with two coordinating pyridyl units and a rotor bearing either a pyridyl or *p*-dimethylaminopyridyl coordinating moiety, the two non-symmetric turnstiles T4 and T5 are based on a stator bearing only a single pyridyl unit and the same rotor as T1 and T2 mentioned above. The switching between the open (T1–T5) and the closed (T-M) states of the turnstiles by metal cations (M = Ag^+ or Pd^{2+}) was investigated in solution by 1D and 2D NMR techniques. The locking of the rotational movement leading the closed state of the turnstile was achieved upon addition of Ag^+ cation through its simultaneous binding by both pyridyl moieties of the stator and to the rotor. The unlocking process leading back to the open state was achieved by addition of Et_4NBr. For the symmetric turnstiles T1 and T2, bearing two pyridyl units on the stator, the binding of Ag^+ cation leads to an oscillating–phenomenon between two energetically equivalent closed states. However, in the case of the turnstile T1, the oscillating process could be prevented by blocking the rotational movement using $PdCl_2$ as the locking agent. Owing to the emissive nature of the stator, the open and closed states of the turnstiles were investigated by steady state and time-resolved photophysical methods. The photo-excitation of the turnstiles in their open state leads to an intense near-UV to deep-blue emission with short-lived excited states and a singlet intra-ligand charge transfer (^{1}ILCT) character. Upon binding of Ag^+ cation, sizeable bathochromic shifts and substantial decrease of PLQY was observed. Finally, coordination of $PdCl_2$, which possesses lower-lying excited states with metal-centered (MC) and ligand-to metal charge transfer (LMCT) character, completely quenches the photoluminescence.

Molecular Tectonics Laboratory, UMR UdS-CNRS 7140, University of Strasbourg, Institut Le Bel, 4, rue Blaise Pascal, F-67000 Strasbourg, France.
Electronic Supplementary Information (ESI) available: full synthetic procedures and characterizations together with 1D and 2D NMR, crystallographic tables and photophysical data. See DOI: 10.1039/x0xx00000x

Introduction

Life is synonymous of motion. Thus, controlled movements and dynamic processes are ubiquitous in living organisms. For example, biological machinery displaying translational movements such as myosin based biomolecular motors[1] or kinesine walkers[2] are among the most studied systems. ATP synthase is one of the most complex and fascinating example of rotary biological motors.[3] It is worth noting that the biological examples mentioned above are large size multi-components complex systems and their design and synthesis are not within reach of synthetic chemistry today. However, over the last two and half decades, based on the pioneering investigations by Sauvage and co-workers[4] and Stoddart, Balzani and co-workers,[5] chemists have investigated a variety of abiotic mobile systems based on individual molecules. Examples reported so far deal with translational or rotational movements induced by an external stimulus such as electrical potential, light and pH, just to cite some.[6] Dealing with rotational systems, Feringa and co-workers reported an elegant design of a chiral molecular motor undergoing directionally controlled movement upon irradiation.[7] In addition to dynamic systems operating in solution, examples of molecular machineries such as gyroscopes in the solid-state have been also reported.[8]

Among the many reported mobile molecular architectures mentioned above, molecular turnstiles form an interesting class of rather simple dynamic entities that are subject to rotational movements.[9] The design of molecular turnstiles is based on two interconnected parts *i.e.* a stator and a rotor. It is worth noting that these two terms may be exchanged since the intramolecular rotational movement engages both parts. This type of molecules undergoes free rotation of the rotor around the stator. In order to setup two different states, one open and the other closed for which the rotational movement is hindered, the turnstile must be equipped with interaction sites located both on the stator and on the rotor. For such molecules, switching between the open and the

View Article Online
DOI: 10.1039/C7DT02762A

closed form can be achieved using an external entity, *i.e.* an effector, able to simultaneously interact with both interaction sites. We have been interested in such dynamic systems for about a decade[10] and designed a variety of molecular turnstiles.[11,12]

In this contribution, we report on the design, synthesis and dynamic behaviour in solution of a series of five symmetric and non-symmetric molecular turnstiles for which switching between an open and closed state has been achieved by binding of a suitable effector (see Figure 1).

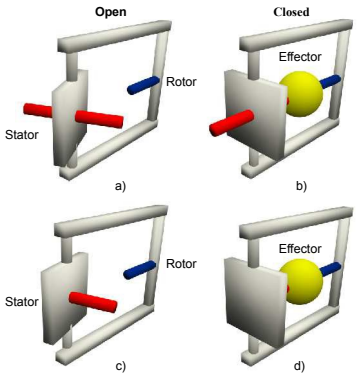

Figure 1. Schematic representations of turnstiles bearing two (a) and one (c) coordinating sites on the stator in their open states and in their closed states (b) and (d) respectively formed upon simultaneous binding of an effector.

Experimental

Experimental details dealing with synthetic procedures, characterization, NMR and photophysical investigations are reported in the Electronic Supplementary Information (ESI) document.

Results and discussion

Design of turnstiles

The design of turnstiles **T1**-**T5** is based on a stator and a rotor connected to the stator by covalent bonds. For all five turnstiles **T1**-**T5**, the same stator based on a hydroquinone scaffold bearing at positions 2 and 5 aromatic moieties is used (see Scheme 1). The rational behind the choice of this unit is based on its luminescent nature that allows monitoring of the switching between the open and closed states by optical reading.[12b]

Turnstiles **T1**-**T3** are based on a symmetric stator, whereas it is non-symmetric for **T4** and **T5**. Indeed, for **T1**-**T3**, it is equipped with either two coordinating pyridyl units (**T1** and **T2**) or two non-coordinating moieties (**T3**). On the other hand, for both **T4** and **T5**, it bears one pyridyl unit as an interaction site and one innocent aryl moiety.

The rotor is composed of an interaction site and two tetraethyleneglycol spacers allowing its connection to the stator. As the coordinating site, either a symmetrically substituted at positions 2 and 6 pyridyl (**T1** and **T4**) or a *para*-dimethylaminopyridyl (**T2**, **T3** and **T5**) moiety is used. The choice of the latter is substantiated by its better coordinating affinity towards metal cations. The two spacers are connected to the interaction site at positions 2 and 6 using ether junctions. Finally, the rotor is connected to the stator again through ether links using positions 1 and 4 of the substituted hydroquinone moiety.

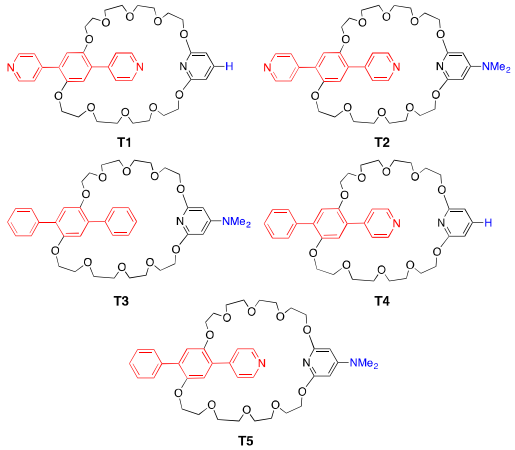

Scheme 1. Chemical structures of molecular turnstiles **T1–T5**. Stator and rotor parts of the molecule are coloured in red and black respectively.

Turnstiles **T1**, **T2**, **T4** and **T5**, all bearing interactions sites on both stator and rotor parts, are designed to undergo a switching process between their open (Fig. 1a and 1c) and closed (Fig. 1b and 1d) states using an external effector such as either Ag^+ or Pd^{2+} cations. Turnstile **T3** is a model compound since it lacks the interaction site on the stator, thus ruling out the possibility to be switched between the two above-mentioned states. The locking of the rotational movement of turnstiles **T1**, **T2**, **T4** and **T5** in the presence of the effector should result from simultaneous binding of the metal cation by both coordinating sites of the stator and the rotor. As previously demonstrated for porphyrin[11a] and Pt(II)[12a] based turnstiles bearing two coordinating groups on the stator, turnstiles **T1** and **T2** are expected to undergo an oscillating movement thus offering two symmetrical closed states. For turnstiles **T4** and **T5**, bearing a single coordinating site (Fig. 1c) on the stator, one would expect a unique closed state (Fig. 1d).

Synthesis of turnstiles

For the synthesis of turnstiles **T1–T5** two different multistep strategies were explored (Scheme 2 and 3).

For the first strategy, the starting material was the commercially available tetraethyleneglycol **1** (Scheme 2). The latter was first mono-activated upon treatment with tosyl chloride (TsCl) using a **1**/TsCl ratio of 10:1 in THF at 0 °C.[13] The derivative **2** then obtained was transformed into **3** in 85% yield upon condensation with 2,6-dibromohydroquinone in presence of K_2CO_3 in refluxing CH_3CN. Compound **3** was treated with an excess of NaH in dry THF over one hour prior addition of 2,6-difluoropyridine. The cyclization process was carried out in dilute condition under reflux. The macrocyclic derivative **4** bearing two bromine atoms was obtained in 12% yield. Subsequently, the two pyridyl units were introduced by a Suzuki coupling reaction between **4** and 4-pyridyl boronic acid in the presence of $Pd(PPh_3)_4$ and Na_2CO_3 as the catalyst and the base, respectively. The reaction was carried out in a mixture of

View Article Online
DOI: 10.1039/C7DT02762A

toluene/methanol at 80 °C affording thus the turnstile **T1** in 69% yield.

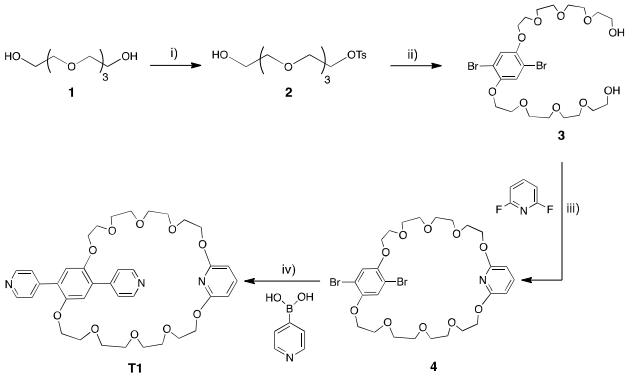

Scheme 2. Synthetic strategy for the preparation of turnstile **T1** (pathway A). Reaction conditions: *i) NaOH, H_2O, tosyl chloride, THF, 0 °C, 4 hours; ii) K_2CO_3, CH_3CN, reflux, 5 days; iii) NaH, THF, reflux, 12 hours; iv) K_2CO_3, $Pd(PPh_3)_4$, toluene/MeOH, 80 °C, 3 days.*

For the synthetic strategy described above, *i.e.* pathway A, the limiting step appeared to be the macrocyclization reaction that proceeds in a rather poor 12% yield. In order to overcome this difficulty, another synthetic pathway was developed, namely pathway B (see Scheme 3). The strategy described above is based first on the functionalization of 2,6-dibromohydroquinone as the precursor of the stator and then the cyclization step using 2,6-difluoropyridine. The second strategy, described below, is the reverse *i.e*. the construction of the rotor and subsequently the cyclisation step. This strategy appeared to be more efficient and allowed preparation of all five turnstiles **T1–T5**.

Tetraethyleneglycol **1** was mono deprotonated using NaH in dry THF and then condensed with either 2,6-difluropyridine **5** or 2,6-difluoro-4-dimethylaminopyridine **6**. The latter was synthetized in 70% yield using a single step procedure by condensation of 2,4,6-trifluoropyridine with dimethylamine.[14] The reaction afforded the desired compounds **7** and **8** in 87% and 81% yield, respectively. The two dihydroxy compounds **7** and **8** were activated as their mesylate derivatives **9** and **10** upon treatment with mesyl chloride (MsCl) in anhydrous THF. The cyclization step was achieved upon condensation of either **9** or **10** with either 2,6-dibromohydroquinone or 2,6-bromoiodohydroquinone in DMF using Cs_2CO_3 as base and afforded the compounds **4**, **11**, **12** and **13** in 77%, 86%, 71%, and 26% yield, respectively. The synthesis of the symmetric turnstiles **T1–T3** was achieved in 69%, 42% and 76% yield, respectively, by Suzuki coupling reaction between either the macrocycle **4** or **11** with 4-pyridyl boronic acid or phenyl boronic acid (Scheme 3). For the non-symmetric turnstiles **T4** and **T5**, a direct strategy based on two Suzuki coupling reactions was required. In order to achieve that, we took advantage of the difference in reactivity between Ar-Br and Ar-I allowing selective functionalization. Thus, macrocyclic derivatives **12** and **13** bearing one bromine and one iodine atom were prepared using 2-bromo-6-iodo-hydroquinone in the macrocyclization step. Compounds **12** and **13** were reacted with 4-pyridinyl boronic acid affording the bromo intermediates **14** and **15** in 63% and 55% yield, respectively. Subsequently, this latter was coupled with phenyl boronic acid to afford the desired asymmetric turnstile **T4** and **T5** in 64% and 80% yield, respectively.

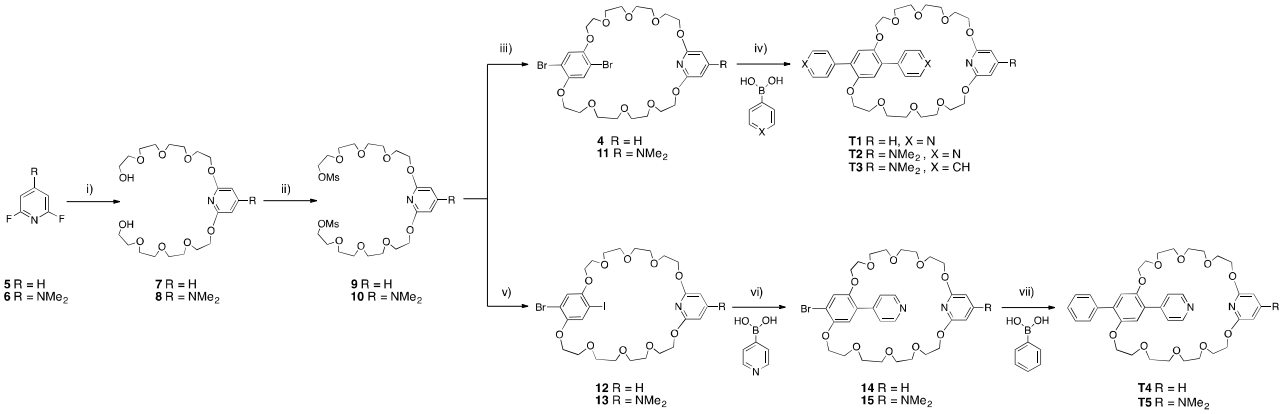

Scheme 3. Schematic general synthetic strategy (pathway B) employed for the preparation of turnstile **1–5**. Reaction conditions: *i) **1**, NaH, THF, reflux, 4 days; ii) mesityl chloride, Et_3N, THF, room temperature, 12 hours; iii) 2,5-dibromohydroquinone, Cs_2CO_3, DMF, 90°C, 24 hours; iv) K_2CO_3, $Pd(PPh_3)_4$, DMF, 100 °C, 48 hours; v) 2-bromo-5-iodohydroquinone, Cs_2CO_3, DMF, 90 °C, 24 hours; vi) K_2CO_3, $Pd(PPh_3)_4$, DMF, 100 °C, 12 hours; vii) K_2CO_3, $Pd(PPh_3)_4$, DMF, 100 °C, 18 hours.*

Among all five turnstiles, single crystals suitable for X-ray diffraction analysis have been obtained only for **T1** so far by slow evaporation of a $CHCl_3$ solution at room temperature (Fig. 2) (see ESI for crystallographic data, CCDC 1565264). The crystal structure (monoclinic, $P12_1/c1$) contained only turnstile molecules. The C–C, C–O and C–N distances are within the expected range for this type of covalent bonds (d = 1.341–1.508 Å). The two $–CH_2O–$ groups connected to the positions 2 and 6 of the pyridyl moiety belonging to the handle are almost coplanar with the heteroaromatic ring (dihedral angles of 1.12 and –5.34°). The two pyridyl units

View Article Online
DOI: 10.1039/C7DT02762A

connected to the stator are not coplanar with the central substituted hydroquinone ring, but tilted by –42.46° and –55.87°.

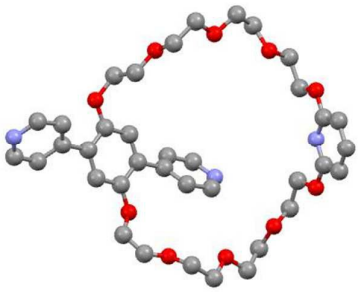

Figure 2. Single crystal X-Ray structure of **T1**. Hydrogen atoms are omitted for sake of clarity. For bond distances and angles see text.

Switching of turnstiles

Turnstiles mentioned above are designed to undergo switching between their open **T**i (i = 1, 2, 4, 5) and closed **T**i-M (i = 1, 2, 4, 5) states in the presence of suitable metal cations as external effector. Indeed, such a switching may be achieved by simultaneous binding of the metal centre by both coordinating sites located on the stator and the rotor (Scheme 4).

At this stage, it is worth noticing that rotational movement can not be blocked by cation addition for **T3** due to the absence of coordinating site on its stator.

As metallic effector, Ag(I) and Pd(II) were used. The choice of Ag^+ cation was based on its affinity to interact with pyridyl units in a reversible manner and its ability to be linearly coordinated. Furthermore, taking advantage of the highly insoluble nature of resulting AgX (X = Cl or Br) salts, the reverse switching from the closed to the open state may be achieved upon addition of halides to the silver complex **T**i-M. The use of *trans*-$PdCl_2(CH_3CN)_2$ as effector was based on its affinity to form stronger complexes with pyridyl bearing ligands and to behave as a linear lock (Scheme 4).

Starting with all four turnstiles **T1**, **T2**, **T4** and **T5** in a mixture of CH_2Cl_2:CH_3CN, the corresponding locked turnstiles **T1**-Ag^+, **T2**-Ag^+, **T4**-Ag^+ and **T5**-Ag^+ were prepared as yellow solids upon treatment with $AgCF_3SO_3$ in the dark, at room temperature. To rule out the role played by the anion on the locking process, in the case of **T1**-Ag^+ and **T2**-Ag^+, the slightly coordinating $CF_3SO_3^-$ anion was replaced by the almost non-coordinating SbF_6^- anion. The NMR investigations in solution (see below) revealed no change in signals chemical shifts upon substitution of $CF_3SO_3^-$ by SbF_6^-.

As previously observed,[12b] the closing of the symmetrical turnstiles **T1** and **T2** affording **T1**-Ag^+ and **T2**-Ag^+ leads to an oscillation phenomena between two equivalent closed states because of the rather weak nature of the Ag-pyridyl bond (see NMR section below). To avoid this dynamic process, the closing process was achieved for turnstiles **T1** and **T5** using $PdCl_2(CH_3CN)_2$ as the locking agent and **T1**-$PdCl_2$ and **T5**-$PdCl_2$ were prepared upon treatment of **T1** and **T5** at room temperature with one equivalent of $PdCl_2(CH_3CN)_2$ in chlorinated solvent (Scheme 4).

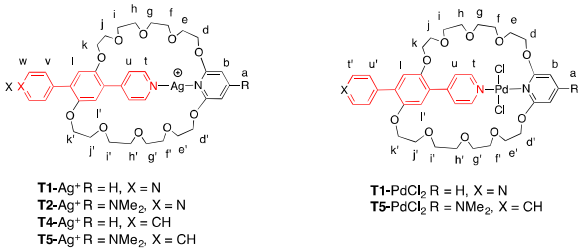

Scheme 4. Chemical structures of molecular turnstile **T1**-Ag^+, **T2**-Ag^+, **T4**-Ag^+, **T5**-Ag^+ and **T1**-$PdCl_2$, **T5**-$PdCl_2$.

Dynamic behaviour of turnstiles

The dynamic behaviour of all five turnstiles was investigated in solution by both 1D and 2D NMR spectroscopies. The choice of different solvents, being CD_3CN, CD_3CN:CH_2Cl_2 9:1 and CD_2Cl_2, was made necessary by the different solubility of the open turnstiles compared to the metal-locked counterparts.

For all five turnstiles **T1**-**T5** and their closed states **T**i-M $^+$ where i = 1-5, all proton signals were assigned by means of ^{1}H- and ^{13}C-NMR (see ESI). For labelling of H atoms see Fig. S1 of the ESI and Scheme 4 for the open and closed state, respectively.

For both **T1** and **T2** the 1D ^{1}H-NMR spectrum recorded in CD_3CN at room temperature displays highly symmetric resonance patterns (see ESI). For the turnstile **T1**, one singlet for the two hydrogens H*l* and H*l'* and one triplet for hydrogen H*a* are observed in the aromatic region. For the turnstile **T2**, the NMR spectrum, recorded under identical conditions, is composed of a singlet in the aromatic region corresponding to H*l* and H*l'* and another singlet at 5.5 ppm assigned to H*b*. The two other doublets in the aromatic region are assigned to H*u*, H*v* and H*t*, H*w*.

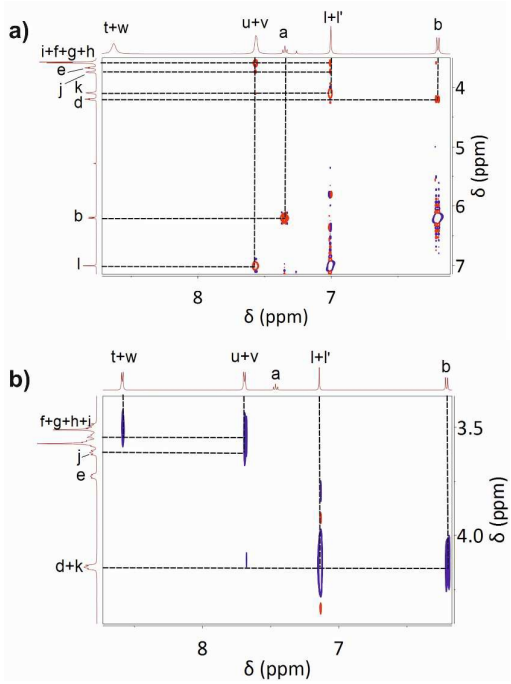

Figure 3. Portion of the 2D NOESY correlations (^{1}H-^{1}H NMR, 400 MHz) for **T1** in $CDCl_3$ (*a*) and **T1**-Ag^+ in CD_3CN (*b*) at 298 K.

View Article Online
DOI: 10.1039/C7DT02762A

The 2D ^{1}H-^{1}H NOESY NMR spectra are displayed in Fig. 3 and in Fig. S2 of the ESI for **T1** and **T2**, respectively. For the turnstile **T1**, the 2D ^{1}H-^{1}H correlation map (Fig. 3a) shows only expected cross-correlations for H atoms located in spatial proximity. Indeed, through-space correlations between H*u* (H*v*) and H atoms of the tetraethyleneglycol chains are observed. A through-space correlation is also observed between H*d* and H*b*. As expected, no through-space correlation between H*t* (H*w*) and H atoms of the tetraethyleneglycol chains are observed owing to the fast rotational movement of the rotor around the stator compared to the NMR time scale. In a similar manner, 2D spectrum of turnstile **T2** shows space correlations between H*u* (H*v*) and hydrogen atoms of the polyethyleneglycol chains and absence of correlation between H*t* (H*w*) and H atoms of the spacer. In addition, H*b* correlates with H*a* and H*d* (see Fig. S2 of the ESI).

The rotational movement of both turnstiles **T1** and **T2** was locked by addition of Ag^+ cations leading to **T1**-Ag^+ and **T2**-Ag^+ complexes. The corresponding NMR characterization is reported in the ESI. As discussed above, the two pyridyl units located on the stator are equivalent because of the symmetrical nature of **T1** and **T2** in their open state. For their closed states, one would expect a lower symmetry resulting from the differentiation of the two pyridyl moieties, *i.e.* only one of the two is bound to the cation. The binding of silver cation causes a downfield shift of signals for H*u* (H*v*) (0.10 ppm for **T1** and 0.16 ppm for **T2**) and for H*l* (H*l'*) (0.12 ppm for **T1** and by 0.28 ppm for **T2**) (see Fig. 4). However, no differentiation of the two pyridyl units is observed since for H*u*, H*v*, H*t* and H*w* only two doublets are observed. The same holds for H*l* and H*l'*. As previously observed for other symmetrical turnstiles bearing two identical coordinating sites on the stator, [10, 12a, 12b] the observed equivalence of the two pyridyl moieties may be explained by a fast oscillation process between two closed states of the same energy.

In order to investigate this dynamic process, variable temperature ^{1}H–NMR studies were carried out between –90 °C and +25 °C in a CD_2Cl_2:CD_3CN 9:1 mixture (see Fig. S3 and Fig. S4 of the ESI). At room temperature, signals corresponding to H*u* (H*v*) and H*t* (H*w*) appear as two sharp doublets (*cf.* above). Upon cooling down to –90 °C, a broadening of signals is observed without their coalescence. Unfortunately, temperature could not be further lowered due to technical reasons. The same behaviour was observed for **T2**-Ag^+ (Figure S4, ESI) between +25 °C and –80 °C.

The oscillating movement was also studied by 2D NMR experiments at room temperature (Fig. 3 and Fig. S2 in ESI). Interestingly, when compared to the 2D ^{1}H-NMR spectra of the open state of **T1** and **T2**, a novel set of correlation appeared for the closed states **T1**-Ag^+ and **T2**-Ag^+ demonstrating the blocking of the movement. Indeed, the observation of through-space correlations between H*t* and H*u* located on the stator and H*f*, H*g*, H*h*, H*i* and H*j* located on the rotor clearly shows the proximity of the pyridyl units to the spacer of the rotor for both oscillating closed states.

The reversibility of the locking/unlocking process was demonstrated by *ex-situ* addition of one equivalent of Et_4NBr in CH_3CN to a CH_2Cl_2 solution of either **T1**-Ag^+ or **T2**-Ag^+, which leads to the precipitation of AgBr. Thus, the unlocking event was followed by ^{1}H-NMR spectroscopy (Fig. 4). Indeed, after evaporation of solvents and dissolution of the reaction product in CD_2Cl_2 the ^{1}H-NMR spectra confirm that the open states of **T1** and **T2** are restored (see traces 3 in Fig. 4).

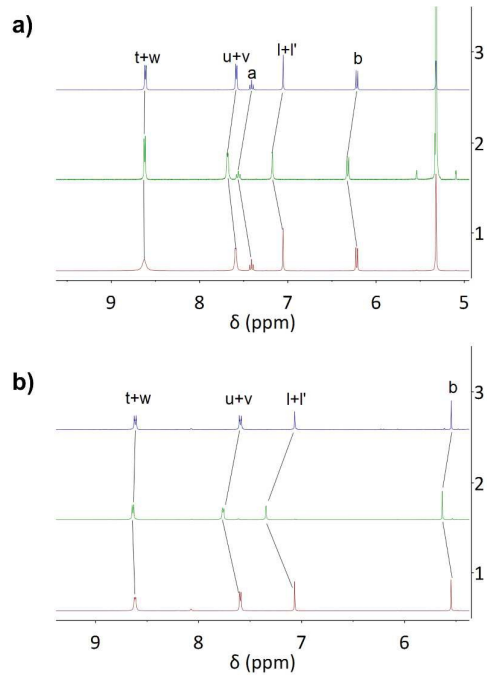

Figure 4. A portion of the ^{1}H-NMR (400 MHz, 298K) spectrum recorded in CD_2Cl_2. *a)* **T1** (trace 1), **T1**-Ag^+ (trace 2) and **T1** after the addition of 1 eq. of Et_4NBr (trace 3). *b)* **T2** (trace 1), **T2**-Ag^+ (trace 2), and **T2** after the addition of one equivalent of Et_4NBr (trace 3). Trace number is indicated along the ordinate axis.

To avoid the oscillating behaviour observed in the presence of Ag^+ cation, Pd(II) as $PdCl_2$ complex was used. The latter was chosen owing to its higher affinity for pyridyl bearing ligands and the less labile nature of the complex. In contrast with what was observed for **T1**-Ag^+, the 1D ^{1}H-NMR investigation of **T1**-$PdCl_2$ (Fig. S7, ESI) clearly showed the differentiation of the free and bound pyridyl units. Indeed, two distinct sets of signals for H*t*, H*u* and H*t'*, H*u'* hydrogen atoms of the pyridyl units are present at room temperature, as expected for a non-dynamic system (see Scheme 4).

The 2D ROESY NMR investigation unambiguously confirmed the non-oscillating nature at room temperature of the closed state of **T1**-$PdCl_2$ (Figure 5). Indeed, a cross-correlation pattern is observed in which H*t* and H*u* hydrogen atoms of the pyridyl moiety bound to Pd(II) correlate with those of the handle. Furthermore, no through space-correlation between H*u'* and H*t'* hydrogen atoms of the unbound pyridyl unit with those of the handle is observed. Moreover, H*l* and H*l'* atoms of the functionalized hydroquinone scaffold, appear as differentiated and display two sets of cross-peak correlations with hydrogen atoms of the stator. Overall, the above mentioned observations clearly indicate that one of the two pyridyl

View Article Online
DOI: 10.1039/C7DT02762A

units of the rotor is engaged in the binding of Pd(II) adopting a square planar coordination geometry.

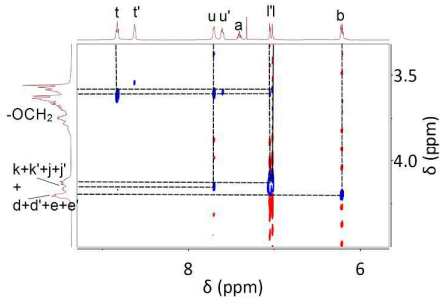

Figure 5. A portion of the ROESY ^{1}H-^{1}H NMR spectrum for **T1**-$PdCl_2$ in CD_2Cl_2 at room temperature.

To suppress the oscillation of **T1**-Ag^+ and **T2**-Ag^+ between two possible degenerate states, two asymmetrically-substituted turnstiles **T4** and **T5** bearing a single pyridyl unit on the rotor were designed and synthetized.

Both **T4** and **T5** were investigated in solution (CD_3CN) at room temperature by 1D ^{1}H-NMR spectroscopy (see ESI). For **T4**, signals corresponding to H*t*, H*u* hydrogen atoms of the pyridyl group and H*v*, H*w*, H*x* of the hydroquinone scaffold appear at 8.58, 7.64 and 7.64, 7.42 and 7.33 ppm, respectively. Signals at 7.46, 7.10 and 7.06 ppm are attributed to H*a*, H*l'* and H*l* H atoms, respectively. Similar chemical shifts are observed for **T5** under identical conditions (for hydrogen assignment see Scheme 4).

As for **T1** and **T2**, the switching between the open and closed state of the unsymmetrical turnstiles **T4** and **T5** was achieved using Ag^+ cation. Addition of one equivalent of $AgCF_3SO_3$ dissolved in CH_3CN to a CH_3CN solution of either **T4** or **T5** caused significant shifts of ^{1}H-NMR signals in particular for signals of the aromatic region of the spectrum. For **T4**-Ag^+, H*u* and H*l'* atoms located on the rotor and H*a* on the stator were downfield shifted by 0.18, 0.08 and 0.05 ppm, respectively. Similar behaviour is observed upon binding of Ag^+ cation to **T5**. However, for the latter case, H*l'* signal appeared to be more affected by the binding silver cation when compared to **T4** because of the higher donating ability of the pyridyl unit bearing a dimethylamino moiety at the position 4 for Ag^+ cation (see ESI).

For turnstiles **T4** and **T5** in their open state, the 2D NOESY investigations (Figure S5 and S6 for **T4** and **T5** respectively, ESI) revealed the presence of correlations between H*t*, H*u* and H*v*. As expected, a correlation between H*a* and H*b* is observed for both **T4** and **T5**. H*v* and H*b* atoms also correlate with H*k*, H*k'* and H*d*, H*d'* H atoms of the handle, respectively. Finally, correlations between H*l'*,H*l* and H*k'* and H*k* atoms are observed. Overall, these observations clearly demonstrate the free rotation of the rotor around the stator.

The closed states of turnstile **T4**-Ag+ and **T5**-Ag+ were also investigated by NMR spectroscopy (for 1H-NMR NOESY spectrum see Figure S5–S6, ESI). For **T4**-Ag^+, correlations between H*t* and H*u* of the rotor with the hydrogen atoms of the stator are observed as expected. Furthermore, H*u* correlates with H*k*. On the other hand, H*v* correlates with nearby hydrogen atoms such as H*k'* and H*j*. Interestingly, H*l* and H*l'* strongly correlate with H*k* and H*k'*, respectively. Finally, a weak correlation peak between H*t* and H*d* is observed. For **T5**-Ag^+, both H*t* and H*u* correlate with hydrogen atoms of the stator. Correlations between H*v* and H*k* as well as between H*b* and H*d*, H*d'* are observed. Finally, H*l'* correlates with the hydrogen atoms of the polyethyleneglycol chains and H*l* correlates only with H*k*. All these observations demonstrate that, upon binding of silver cation by both the pyridyl unit of the rotor and the one of the stator, the latter is located within the cavity of the macrocyclic moiety.

Photophysical investigation

The open state of turnstiles **T1**-**T5** and their closed states formed upon binding of either Ag^+ or Pd^{2+} cations are expected to possess different optical properties. Indeed, the binding of metal cations by the pyridyl coordinating units should affect both nature and energy levels of the excited states. The steady-state and time-resolved photophysical properties of turnstiles **T1**-**T5** and their metal complexes **Ti**-Ag^+ (**i** = 1–5) as well as **T1**-$PdCl_2$ have been investigated in dilute solution at room temperature and the photophysical data are listed in Table 1.

Table 1. Photophysical data recorded at room temperature for **Ti, Ti**-Ag^+ (where **i** = 1–5), and **T1**-$PdCl_2$ in CH_3CN at 1.0×10^{-5} M concentration.

sample	absorbance (ε) [nm, (10^3 $M^{-1}cm^{-1}$)]	λ_{em} [nm]	lifetime [ns]	PLQY (%)
T1	275 (23.1), 334 (8.7)	415	4.1 [a]	57
T2	267 (18.4), 334 (8.1)	415	4.8 [a]	36
T3	269 *sh* (19.8), 319 (10.1)	384	1.8 [a]	31
T4	275 (22.1), 327 (9.6)	405	3.3 [a]	67

View Article Online
DOI: 10.1039/C7DT02762A

T5	269 *sh* (17.7), 327 (9.4)	405	3.3 [a]	42
T1-Ag^+	275 (19.2), 335 (6.8), 400*sh* (0.5)	415[a] 546[b]	4.2 λ_{em} = 415 (air) [a] 1.6 λ_{em} = 532 (air) [c] 4.9 λ_{em} = 415 (deg) [a] 1.9 λ_{em} = 545 (deg) [c]	12 (air) [a]
T2-Ag^+	266 (15.3), 344 (4.2), 385*sh* (2.2)	415, 535*sh* [a] 534[b]	4.7 (75%), 1.0 (25%) λ_{em} = 415 (air) [a] 2.7 λ_{em} = 532 (air) [c] 1.2 (31%) λ_{em} = 415 [a] 6.0 (69%) λ_{em} = 415 [a] (deg) 1.6 (17%), 3.0 (83%) λ_{em} = 532 [c] (deg)	6 (air) [a]
T3-Ag^+	269 *sh* (10.05), 319 (7.5)	383 [d]	1.7 [a]	28 [d]
T4-Ag^+	275 (22.8), 325 (9.5),380 *sh* (1.8)	404, 533 *sh*[d] 550[b]	3.3 λ_{em} = 405 (air) [a] 1.2 λ_{em} = 550 (air) [c]	41[d]
T5-Ag+	269 *sh* (21.8), 306 (9.05), 376 *sh* (4.8)	405, 528 *sh*[d] 539[b]	3.4 λ_{em} = 405 (air) [a] 2.1 (69%) λ_{em} = 550 (air) [c] 1.3 (31%) λ_{em} = 550 (air) [c]	28[d]
T1-$PdCl_2$	275 (10.6), 335 (4.4), 400*sh* (1.1)	–	–	–

sh denotes a shoulder; [a] λ_{exc} = 340 nm; [b] λ_{exc} = 400 nm; [c] λ_{exc} =370, [d] λ_{exc} =320 nm.

The electronic absorption spectra of turnstiles **T1**–**T5** in CH_3CN are displayed in Figure 6. At shorter wavelength, all the investigated samples display a narrow and intense (ε = 1.8–2.3 $\times 10^4$ M^{-1} cm^{-1}) absorption band centred at λ_{abs} *ca.* 270 nm that can be ascribed to a transition with spin-allowed singlet-manifold ligand centred (^{1}LC) character. At longer wavelengths in the region 320–340 nm, the spectra show a featureless absorption band with lower intensity (ε = 1.0–0.8 $\times 10^4$ M^{-1} cm^{-1}) that can be ascribed to an ^{1}ILCT transition involving the π-conjugated phenylene-*bis*-pyridyl system located on the stator.

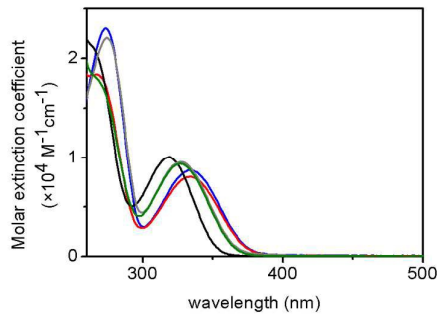

Figure 6. UV-visible absorption spectra of turnstiles **T1** (blue trace), **T2** (red trace), **T3** (black trace), **T4** (grey trace) and **T5** (green trace) at concentration of 1.0×10^{-5} M in CH_3CN at room temperature.

View Article Online
DOI: 10.1039/C7DT02762A

The partial charge transfer (CT) nature of the lowest-lying electronic transition has been confirmed by solvent effect study in the case of **T1**, which shows a slight bathochromic shift of the absorption maximum upon increasing solvent polarity (see Table 2). For spectra recorded in toluene, CH_2Cl_2, CH_3CN and DMF at identical dilution of 1.0×10^{-5} M see Fig. S8 in the ESI.

Table 2. Electronic absorption data recorded for **T1** in different solvents.

Solvent	Absorbance (ε) [nm, (10^3 $M^{-1}cm^{-1}$)]
toluene	332 (8.32)
CH_2Cl_2	334 (7.34)
CH_3CN	335 (8.7)
DMF	338 (8.53)

As shown in Fig. 7, upon photo-excitation (λ_{exc} = 310–350 nm) of samples of **T1–T5** in dilute CH_3CN at room temperature, an intense (PLQY = 31–67%) emission in the violet to deep-blue region was observed with featureless and narrow profile and moderate Stokes shift (5300–5890 cm^{-1}). Excited state lifetime measurements showed mono-exponential decay kinetics with τ = 1.8–4.8 ns. Modulation of the emission maximum was observed with a sizeable bathochromic shift going from **T3** to **T4–T5** to **T1–T2**, as consequence of the increased π-accepting ability of the pyridyl fragment compared to phenyl moiety of the stator, *i.e.* where the emitting excited state is expected to be located. Such substituent effect mirrors the modulation observed in the lowest-lying absorption and emission maxima (see Fig. 6–7). On the basis of these observations, the emission can be described as arising from an excited state with ^{1}ILCT character.

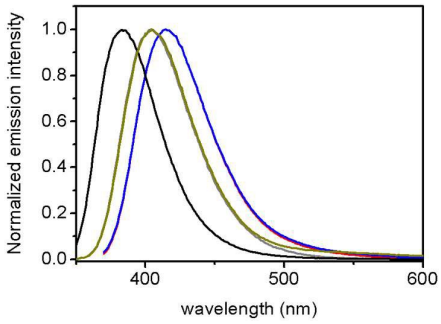

Figure 7. Normalized emission spectra for sample of **T1** (blue trace), **T2** (red trace), **T3** (black trace), **T4** (grey trace) and **T5** (green trace) in dilute CH_3CN at room temperature upon excitation at λ_{exc} = 320 nm.

The photophysical properties of turnstiles in their closed form, namely **Ti**–Ag^+ (**i** = 1–5) and **T1**–$PdCl_2$, were measured as well and the corresponding spectra are displayed in Fig. 8 for **T1**–Ag^+, **T2**–Ag^+ and **T1**–$PdCl_2$, and Figure S10-S12 of the ESI for **T3**–Ag^+, **T4**–Ag^+ and **T5**–Ag^+. The photophysical data are also listed in Table 1. For the Ag^+-locked turnstiles, besides the intense (ε = 4.2–6.8 $\times10^3$ M^{-1} cm^{-1}) ^{1}ILCT band centred at 335 and 344 nm for **T1**–Ag^+ and **T2**–Ag^+, respectively, appearance of a novel and less intense absorption process attributable to a metal-perturbed ^{1}ILCT process is clearly visible as a shoulder in the lower-energy region of the spectrum. This results from silver coordination by the two pyridyl moieties located on both rotor and stator sites. Such lower energy band is more intense for **T2**–Ag^+ than for **T1**–Ag^+ most likely because of the more electron donor character of the rotor pyridyl unit bearing an electron donor dimethylamino moiety at the *para* position. Likewise, a sample of **T1**–$PdCl_2$ in CH_3CN displays an electronic absorption onset that lies at further lower energy compared to **T1**–Ag^+ and most likely arising from a transition with ligand-to-metal charge transfer (^{1}LMCT) character, *i.e.* π(pyridine)$\rightarrow$dπ^*(Pd) on the basis of related Pd(II) complexes reported elsewhere.[15] A rather similar picture can be drawn for the other derivative **T3**–Ag^+, **T4**–Ag^+ and **T5**–Ag^+ (see ESI).

Upon excitation at λ_{exc} = 340–400 nm, **T3**–Ag^+ showed photoluminescence features that are similar to what observed for its open counterpart **T3** in terms of emission profile, excited state lifetime and PLQY, as expected on the basis of its chemical design, (Fig. S10 and Table 1). On the other hand, **T1**–Ag^+ and **T2**–Ag^+ displayed a dual band emission profile with maxima centred at 415 nm for both derivatives that corresponds to the emission observed for the free **T1** and **T2** (see above). The second and much less intense emission band is centred at 546 and 534 nm, for **T1**–Ag^+ and **T2**–Ag^+, respectively. These bands are attributable to the metal-perturbed ^{1}ILCT of the closed form of the turnstile owing to the presence of the coordinated metal ion.[16] Indeed, this lower energy emission band appears more pronounced when samples were excited at 400 nm, *i.e.* when the lowest-lying ^{1}ILCT absorption band of the closed form is preferentially excited, as shown in Fig. S9 of the ESI. Upon excitation at 340 nm, the overall emission intensity was moderate, being the PLQY of 12% and 6% for **T1**–Ag^+ and **T2**–Ag^+, respectively. The origin of such dual emission stems from the fact that in solution at least two possible luminescent species, *i.e.* **T1** or **T2** and **T1**–Ag^+ or **T2**–Ag^+, respectively, may coexist in a dynamic equilibrium resulting from the rather low binding constants for the complexation of silver cation. Moreover, the CT character of such radiative process is confirmed by substituent effect as demonstrated by the hypsochromic shift observed in the emission spectra of **T2**–Ag^+ when compared to **T1**–Ag^+, as a consequence of the stabilisation effect exerted by the more donating NMe_2-pyridine moiety in **T2**–Ag^+, while keeping the lowest-lying π-accepting pyridine on the stator (*i.e.*, the LUMO level) at the same energy. The dual nature of such emission profile was further confirmed by time-resolved measurements that showed a wavelength-dependent bi-exponential decay with long and short component being $\boldsymbol{\tau_1}$= 6.0 ns (69%) and τ_2 = 1.2 ns (31%), and τ_1 = 3.0 (83%) and τ_2 = 1.6 (17%), for degassed samples of **T2**–Ag^+ recorded at 415 and 532 nm, respectively, attributable to the open and closed form of the turnstile present in solution (see Table 1). Also, in spite of the presence of the heavy metal which may provide a partial triplet nature to the excited states, lifetimes of these latter appeared to be insensitive to the presence of quenching dioxygen molecules as expected for a fast radiative deactivation processes under diffusion control (see Table 1). Similar

View Article Online
DOI: 10.1039/C7DT02762A

findings were found for derivative **T4**–Ag^+ and **T5**–Ag^+ (see Fig. S11-S12 of the ESI and Table 1).

Upon photo-excitation at 340–400 nm no emission was detected for **T1**–$PdCl_2$ as one may expect due to the presence of lowest-lying quenching excited states with either *d-d* or LMCT character. The latter case is interesting since, as already exploited,[17] it further demonstrates the possibility of optical reading between the open (**T1**) and closed (**T1**–$PdCl_2$) states of the turnstiles **T1**.

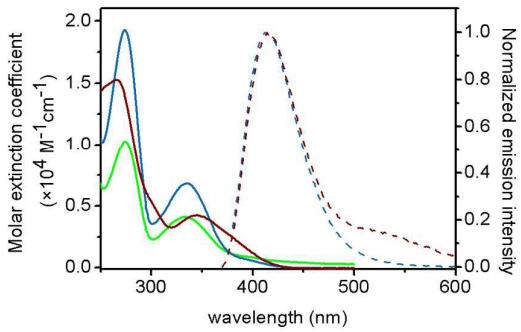

Figure 8. UV-visible absorption (solid traces) and emission spectra (dashed traces) of samples of turnstile **T1**-Ag^+ (light blue), **T2**-Ag^+ (bordeaux) and **T1**-$PdCl_2$ (light green) at concentration of 1.0×10^{-5} M in CH_3CN at room temperature. Emission spectra were recorded upon λ_{exc} = 340 nm in degassed condition.

Conclusions

The synthesis of a novel family of molecular turnstiles based on either a symmetric or non-symmetric stator equipped with pyridyl unit and a rotor bearing either a pyridyl or *p*-dimethylamino pyridyl coordinating moiety was achieved. The switching between the open and the closed states of the turnstiles by metal cations (Ag^+ or Pd^{2+}) was investigated in solution by 1D and 2D NMR techniques. The locking of the rotational movement of the turnstiles was achieved upon simultaneous binding of Ag^+ cation by both pyridyl moieties belonging to the stator and to the rotor. The locking process is reversible and the open state may be regenerated upon addition of Et_4NBr leading to the precipitation of AgBr. For the symmetric turnstiles **T1** and **T2** bearing two pyridyl units on the stator the binding of Ag^+ cation expectantly leads to an oscillating phenomena between two closed states of the same energy as demonstrated by 1D and 2D NMR techniques. In marked contrast, in the case of the turnstile **T1**, the oscillating process could be altered by blocking the rotational movement using $PdCl_2$ as the locking agent. Finally, the open and closed states of turnstiles **T1**-**T5**, based on an emissive stator, *i.e.* a hydroquinone moiety bearing at positions 2 and 5 aromatic units, were investigated by steady state and time-resolved photophysical methods. In solution and upon photo-excitation, turnstiles in their open state show intense near-UV to deep blue emissions with short-lived excited states and a ^{1}ILCT character. Upon binding of Ag^+ cation, sizeable bathochromic shifts and substantial decrease of PLQY are observed for **Ti** (**i** = 1, 2, 4 and 5). Expectantly, similar photophysical properties were observed for model compound **T3** before and after addition of Ag^+ ions. Finally, coordination of $PdCl_2$, which possess lower-lying excited states with MC and LMCT character, completely quenches the photoluminescence allowing thus the ON/OFF reading of the locking process by luminescence.

Acknowledgements

We thank the University of Strasbourg, the C.N.R.S., the International centre for Frontier Research in Chemistry (icFRC), the Labex CSC (ANR-10-LABX- 0026 CSC) within the Investissement d'Avenir program ANR-10-IDEX-0002-02, the Institut Universitaire de France and the Ministère de l'Enseignement Supérieur et de la Recherche for financial support and a scholarship to BG.

Notes and references

1 a) J. T. Finer, R. M. Simmons, J. A. Spudich, *Nature* 1994, **368**, 113–119; b) M. Whittaker, E. M. Wilson-Kubalek, J. E. Smith, L. Faust, R. A. Milligan, H. L. Sweeney, *Nature*, 1995, *378*, 748–751.

2 a) E. P. Sablin, F. J. Kull, R. Cooke, R. D. Vale, R. J. Fletterick, *Nature* 1996, **380**, 555–559; b) E. Meyhofer, J. Howard, *Proc. Natl. Acad. Sci*, 1995, **92**, 574-578.

3 a) T. Elston, H. Y. Wang, G. Oster, *Nature* 1998, **391**, 510–513; b) H. Noji, R. Yasuda, M. Yoshida, K. Kinosita, *Nature* 1997, **386**, 299–302.

4 a) J. P. Sauvage, *Acc. Chem. Res*. 1998, **31**, 611−619; b) J. P. Sauvage, *Science* 2001, **291**, 2105−2106; c) J. P. Sauvage, in Molecular Machines and Motors, Springer: Berlin, Heidelberg, 2001; Vol. 99, pp 1−282.

5 a) P. R. Ashton, R. Ballardini, V. Balzani, I. Baxter, A. Credi, M. C. T. Fyfe, M. T. Gandolfi, M. Gómez-López, M. V. Martínez-Díaz, A. Piersanti, N. Spencer, J. F. Stoddart, M. Venturi, A. J. P. White, D. J Williams, *J. Am. Chem. Soc*. 1998, **120**, 11932−11942; b) C. J. Bruns and J. F. Stoddart, The nature of the mechanical bond, Wiley, 2017.

6 a) V. Balzani, M. Venturi, A. Credi, In Molecular Devices and Machines: a Journey into the Nanoworld; Wiley-VCH: Weinheim, 2003; b) V. Balzani, M. Gomez-Lopez, J. F. Stoddart, Molecular Machines. *Acc. Chem. Res*. 1998, **31**, 405-414; c) R. A. van Delden, M. K. J. ter Wiel, N. Koumura, B. L. Feringa in Molecular Motors (Ed.: M. Schliwa), Wiley-VCH, Weinheim, 2003, pp. 559-577; d) W. R. Browne, B. L. Feringa, *Nat. Nanotechol*., 2006, **1**, 25-35; e) T. R. Kelly, Molecular machines, *Top. Curr. Chem*. Springer, Berlin, Heidelberg, 2005, **262**, 1-227; f) E. R. Kay, D. Al. Leigh, F. Zerbetto, *Angew. Chem. Int. Ed*., 2007, **46**, 72-191; g) G. S. Kottas, L. I. Clarke, D. Horinek, J. Michl, *Chem. Rev.*, 2005, **105**, 1281-1376; h) G. Vives, H.-P. Jacquot de Rouville, A. Carella, J.-P. Launay and G. Rapenne, *Chem. Soc. Rev.*, 2009, **38**, 1551-5161; i) K. Tashiro, K. Konishi and T. Aida, *J. Am. Chem. Soc.*, 2000, **122,** 7921-7926; j) K. Kinbara, T. Muraoka and T. Aida, *Org. Biomol. Chem*., 2008, **6**, 1871-1876; k) M. Takeuchi, T. Imada and S. Shinkai, *Angew. Chem. Int. Ed.*, 1998, **37**, 2096-2099; l) J. F. Morin, Y. Shirai and J. M. Tour, *Org. Lett*., 2006, **8**, 1713-1716; m) I. Pochorovski, M. O. Ebert, J. P. Gisselbrecht, C. Boudon, W. B. Schweizer and F. Diederich, *J. Am. Chem. Soc.*, 2012, **134**, 14702-

View Article Online
DOI: 10.1039/C7DT02762A

14705; n) E. Busseron, C. Romuald and F. Coutrot, *Chem. Eur. J.*, 2010, **16**, 10062-10073; o) C. Clavel, C. Romuald, E. Brabet, F. Coutrot, *Chem. Eur. J.*, 2013, **19**, 2982-2989.

7 a) N. Koumura, R. W. J. Zijlstra, R. A. van Delden, N. Harada, B. L. Feringa, *Nature* 1999, **401**, 152 –155; b) M. K. J. ter Wiel, R. A. van Delden, A. Meetsma, B. L. Feringa, *J. Am. Chem. Soc*. 2003, **125**, 15076 – 15086.

8 a) M. A. Garcia-Garibay, C. E. Godinez, *Cryst. Growth Des*., 2009, **9**, 3124-3128; b) A. Comotti, S. Bracco, P. Sozzani, *Acc. Chem. Res.*, 2016, **49**, 1701-1710.

9 a) T. C. Bedard and J. S. Moore, *J. Am. Chem. Soc.,* 1995, **117**, 10662-10671; (b) A. Carella, J. Jaud, G. Rapenne and J.-P. Launay, *Chem. Commun.,* 2003, 2434-2435; (c) N. Weibel, A. Mishchenko, T. Wandlowski, M. Neuburger, Y. Leroux and M. Mayor, *Eur. J. Org. Chem.,* 2009, **35**, 6140-6150; (d) K. Skopek, M. C. Hershberger and J. A. Gladysz, *Coord. Chem. Rev.,* 2007, **251**, 1723-1733; e) P. D. Zeits, G. P. Rachiero, F. Hampel, J. H. Reibenspies, J. A. Gladysz, *Organometallics*, 2012, **31**, 2854-2877.

10 A. Guenet, E. Graf, N. Kyritsakas, L. Allouche, M. W. Hosseini, *Chem. Commun*., 2007, 2935-2937.

11 a) T. Lang, A. Guenet, E. Graf, N. Kyritsakas, M. W. Hosseini, *Chem. Commun*., 2010, **46**, 3508-3510; b) A. Guenet, E. Graf, N. Kyritsakas, M. W. Hosseini, *Chem. Eur. J.*, 2011, **17**, 6443-6452; c) I. N. Meshkov, V. Bulach, Y. G. Gorbunova, N. Kyritsakas-Gruber, M. S. Grigoriev, A. Y. Tsivadze, M. W. Hosseini, *Inorg. Chem*, 2016, **55**, 10774 –10782.

12 a) N. Zigon and M. W. Hosseini, *Chem. Commun*., 2015, **51**, 12486-12489; b) N. Zigon, P. Larpent, A. Jouaiti, N. Kyritsakas and M. W. Hosseini, *Dalton Trans*, 2014, **43**, 15779-15784.

13 K. D. Park, R. Liu, H. Kohn, *Chem. Biol*., 2009, **16**, 763-772.

14 L. J. Kershaw Cook, R. Kulmaczewski, R. Mohammed, S. Dudley, S. A. Barrett, M. A. Little, R. J. Deeth, and M. A. Halcrow, *Angew. Chem. Int. Ed*., 2016, **55**, 4327-4331.

15 S. Zhang, R. Pattacini, P. Braunstein, L. De Cola, E. Plummer, M. Mauro, C. Gourlaouen, C. Daniel, *Inorg. Chem*., 2014, **53**, 12739-12756.

16 a) C. W. Hsu, C. C. Lin, M. W. Chung, Y. Chi, G. H. Lee, P. T. Chou, C. H. Chang and P. Y. Chen, *J. Am. Chem. Soc*., 2011, **133**, 12085–12099; b) A. Barbieri, G. Accorsi and N. Armaroli, *Chem. Commun*., 2008, **19**, 2185–2193.

17 N. Zigon, P. Larpent, A. Jouaiti, N. Kyritsakas, M. W. Hosseini, *Chem. Commun*., 2014, **50**, 5040-5042.

View Article Online
DOI: 10.1039/C7DT02762A

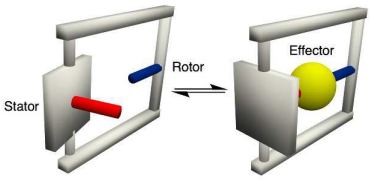

Luminescent symmetrical and non-symmetrical molecular turnstiles based on hydroquinone stators and rotors bearing pyridyl or *p*-dimethyaminopyridyl coordinating units